DISCLAIMER

This report was prepared as an account of work sponsored by an agency of the United States Government. Neither the United States Government nor any agency thereof, nor any of their employees, makes any warranty, express or implied, or assumes any legal liability or responsibility for the accuracy, completeness, or usefulness of any information, apparatus, product, or process disclosed, or represents that its use would not infringe privately owned rights. Reference herein to any specific commercial product, process, or service by trade name, trademark, manufacturer, or otherwise does not necessarily constitute or imply its endorsement, recommendation, or favoring by the United States Government or any agency thereof. The views and opinions of authors expressed herein do not necessarily state or reflect those of the United States Government or any agency thereof. Reference herein to any social initiative (including but not limited to Diversity, Equity, and Inclusion (DEI); Community Benefits Plans (CBP); Justice 40; etc.) is made by the Author independent of any current requirement by the United States Government and does not constitute or imply endorsement, recommendation, or support by the United States Government or any agency thereof.

SANDIA REPORT
SAND2025-09228
Printed July 25, 2025

Sandia National Laboratories

A Short Survey of Current Reactive Burn Model Capabilities as of Mid-Year 2025

David E. Kittell, Antonio R. Garcia, Michael L. Hobbs, William W. Erikson, Kevin P. Ruggirello, Judith A. Brown, David L. Damm, James A. Stewart, Peter A. Sable, Jeffrey W. LaJeunesse, Eric N. Harstad, Leah W. Tuttle, and Aaron L. Brundage

Prepared by
Sandia National Laboratories
Albuquerque, New Mexico 87185
Livermore, California 94550

Issued by Sandia National Laboratories, operated for the United States Department of Energy by National Technology & Engineering Solutions of Sandia, LLC.

Available to DOE and DOE contractors from

U.S. Department of Energy
Office of Scientific and Technical Information
P.O. Box 62
Oak Ridge, TN 37831

Telephone: (865) 576-8401
Facsimile: (865) 576-5728
E-Mail: reports@osti.gov
Online ordering: http://www.osti.gov/scitech

Available to the public from

U.S. Department of Commerce
National Technical Information Service
5301 Shawnee Road
Alexandria, VA 22312

Telephone: (800) 553-6847
Facsimile: (703) 605-6900
E-Mail: orders@ntis.gov
Online order: https://classic.ntis.gov/help/order-methods

ABSTRACT

The authors were tasked with writing a concise memo (now a short report) that adequately addresses the current "state-of-the-art" in the field of reactive flow modeling and burn models for mid-year 2025, along with identifying some of the modeling gaps. It is assumed that the reader has experience with burn models and running hydrocode simulations, and thus every effort is made to ensure brevity, clarity, and utility, so that this document will serve as a quick and useful reference. Note that "mid-year" was used in the title, as it is possible that advancements in artificial intelligence (AI) may significantly impact the field before the year is over.

QUALIFICATIONS FOR WRITING

The authors are not the first to summarize the history of burn models, nor do they represent the opinions of Sandia, nor of any other U.S. DOE weapons laboratory. Burn models were created over many decades, notably by Mader [1], and there exist recent review papers (e.g., [2],[3]) which delve into greater details. However, the authors are subject matter experts at Sandia who routinely exercise reactive flow model capabilities, especially in CTH. The lead author has published journal papers on fitting reactive flow models [4],[5], and recently delivered a plenary talk at the Seventeenth International Detonation Symposium concerning the CREST reactive burn model [6].

ORGANIZATION AND FORMAT

The format of this memo consists of short paragraphs organized by topic, with minimal figures. The authors took inspiration from a 20-page report written by Proud [7] for NATO, entitled "Ignition and Detonation in Energetic Materials: An Introduction," which strikes an excellent balance between depth and breadth. In the current report, most of the burn model details may be found in the citations, unless it is necessary to show the details here.

CONTENTS

LIST OF FIGURES

1. CONTEXT FOR BURN MODELS

1.1. Intended usage

Originally, burn models were developed to simulate the processes involved with a shock to detonation transition (SDT) in high explosives (HEs). When an analyst knew that an explosive was going to detonate, then he or she would use a programmed burn model. If an analyst did not know if or when an explosive was going to detonate, then (and only then) would they consider using a reactive burn model. **It is only in recent times that burn models are tasked to represent the full range of shock and detonation phenomena observed in HEs [3]**.

Another way to think about the context for burn models was often said to us by the late Bob Schmitt, Sandia National Laboratories (SNL), by way of asking a question, as follows:

- **Do you care about what is happening on the inside of an explosive, as it is shocked?** If 'yes,' then consider using a reactive burn model in the calculation. Within the scope of the modeling communities studying engineering applications and design, reactive burn models are considered to be "high-fidelity" models.

- **Do you care about what the explosive is doing to its surroundings**, e.g., pushing metal or making fragments? If 'yes,' then consider using a fast-running model such as programmed burn. Fast-running models are also an active area of research in the same way that reactive burn models are.

Sometimes we care about both the internal behavior and the external effects of the detonation. Unfortunately, the chemical length scales of reaction (which require burn models) can be orders of magnitude smaller than the hydrodynamic length scales of fast-running models. Therefore, one must choose which of these length scales is the most important–it is computationally prohibitive to design a simulation that resolves an HE at a fine mesh resolution for burn models, but that also encompasses an entire device in the computational domain, with hundreds of grams to kilograms of HE, and upwards of one billion elements or cells. It is unlikely for this situation to change any time soon, even with the investments in exascale computing.

1.2. The costly nature of using burn models

While most burn models are phenomenological, they are also "high-fidelity" in many ways, increasing both the simulation run times and central processing unit (CPU) resources for an otherwise inert shock simulation. These models close the set of governing conservation equations for mass, momentum, energy, and species (i.e., reactants going to products) together with equations of state (EOS) for the solid HE, detonation products, and partially reacted HE. In addition, there is a rate law, in the form of a differential equation, to advance the reactants to products. Of these "ingredients," the EOS are usually well calibrated, so only the rate law is phenomenological (it

is empirical, really); the associated differential equations are stiff, and so they contribute to the increased computational costs, along with finer mesh resolutions required to run these models.

1.3. Fast-running models for large calculations

Unlike reactive burn models, there also exists a class of fast-running models that are typically employed when simulating and designing full-scale munitions and HE devices that are expected to detonate. Programmed burn is one such example, which assumes a fixed detonation velocity, D_{CJ}, and then calculates the trajectory of the detonation wave in multiple dimensions via a level set algorithm, Huygens' construction, or similar approach [8].

There are other fast-running models with improved fidelity, most notably the Los Alamos National Laboratory (LANL) detonation shock dynamics (DSD) approach [9]. In DSD, the simple Huygens' construction is relaxed to allow for variations in detonation wave speed, resulting in more accurate time of arrival (TOA) predictions in components with complicated geometries. We note, Aslam has published recent work on an advanced DSD model (2024) [10].

Fast-running models have gained significant attention in recent years, but they have yet to be updated in most of the legacy hydrocodes. Also, they cannot be used to simulate SDT, so one must know ahead of time that an HE will detonate. Looking towards the future in this area, there is Stewart's eigenvalue detonation model (2024) [11],[12], which could pave the way for fast-running models for non-ideal explosives, including ammonium nitrate and fuel oil (ANFO) and aluminized blast explosives.

1.4. Burn models are associated with heterogeneities

Throughout the history of burn models, beginning with Forest fire (which was named after Charles Forest at Los Alamos, and not the ecological disasters) [13] and Ignition and Growth [14], there has always been an implicit connection made between the rate law, HE microstructures, and the formation of localized areas of elevated temperature know as 'hot spots.' This is somewhat unfortunate for the homogeneous gaseous and liquid explosives, which do not rely on hot spots to transition to detonation, but are also simulated using so-called "burn models."

Nevertheless, heterogeneities and hot spots are by far the most common realities when studying SDT in HEs, and so the implicit connections remain unchanged. Menikoff and Shaw [13] make an excellent statement in their introduction about solid HEs and burn models:

"Though heterogeneous, an HE is modelled as homogeneous, and an 'effective' burn rate, rather than a chemical rate, is used to account for unresolved physical phenomena; namely, temperature fluctuations on the spatial scale of the heterogeneities that arise when an HE is subject to a strong compressive wave. The temperature fluctuations result in local hot spots that dominate the reaction, and are critical for ignition."

1.5. Legacy burn models were fit to Pop plot data

The very first burn models for solid HEs were fit to one-dimensional SDT data consisting of time-to-detonation, t_d, distance-to-detonation, x_d, and the initial shock pressure, P_0, from wedge tests. These quantities were plotted on a log-log plot in distance or time versus pressure, known as a Pop plot, after Alphonse Popolato [15],[16]. In particular, the quintessential Pop plot is a least squares fit of the form $\ln(x_d) = a + b \ln(P_0)$ to the sustained shock initiation data.

While Pop plot data was (and still is) critical for parameterizing the legacy models, a few comments are the following: **(1)** there was a gap in time, somewhere between 10-20 years, from the maturation of the experiments, to the maturation of the burn models, **(2)** fitting Pop plot data is necessary but not sufficient for parameterizing burn models, as there is no measurement of the buildup to detonation, and finally **(3)** large scale wedge tests are no longer conducted at LANL, at least in the same manner.

2. STATE-OF-THE-ART BURN MODELS

2.1. Fit all of the experiments (...reasonably well)

As mentioned in Sec. 1.5, wedge tests are no longer conducted in the same manner at LANL. Sometimes, legacy Pop plot data is available, and it is included in the burn model calibration suite. Otherwise, the best SDT data comes from embedded particle velocity gauge measurements, from gas gun launched flyer impact experiments [17]. Not only does Lagrangian particle velocity data provide a more rigorous challenge for burn models to match, but the impact conditions may be varied, and the projectile may be modified to obtain double-shock, thin pulse, and shock-release-reshock experiments as well.

Beyond these gas gun experiments, modern burn models are now calibrated using two-dimensional curved flyer impacts (e.g., laser launched or round nose projectiles) [18], transverse initiation experiments [19], corner turning experiments [20], uncased or bare rate stick detonation studies [21], gap stick experiments [22], disc acceleration eXperiment (DAX) [23], and many others such as high-throughput initiation (HTI) [24] – space limitations do not permit us to discuss them all here. No single burn model fits all of the available data exactly; the best burn models fit the data well enough to make reasonable predictions.

2.2. Did not fall by the wayside, while others did

It is interesting to consider the legacies of the original LANL Forest fire model [13] developed in the 1970's, and the Lawrence Livermore National Laboratory (LLNL) Ignition and Growth (I&G) model developed in the 1980's [14]. The addition of a third term (and lots of parameters!) to I&G allowed the LLNL model to fit a wider range of experiments, while the LASL Forest fire model

was too simplistic and fitted only Pop plot data. An addendum to Forest fire was published several years later; however, before then, other models began to replace Forest fire in prominence. During these early years, two other LANL models called DAGMAR and JTF appeared on the scene, with reaction rate laws that were based on the lead (i.e., captured) shock pressure. These models never gained favor, due in part to numerical issues with robustness [2].

History is the best judge of which burn models are successful. Typically, each burn model has its champion, who is responsible for promoting the model (i.e., educating analysts and decision-makers) and insuring its transition and legacy. To this end, the best burn models are available in production hydrocodes, and the mathematical expressions do not exceed the understanding of an experienced analyst or researcher in the field.

2.3. Are household names within the community

All of the "state-of-the-art" burn models are easily recognizable via their publication records and authorship. Following the Seventeenth International Detonation Symposium (IDS), Kansas City, MO, August 4–9, 2024, one can glean which burn models are in widespread use in the U.S. over the 2024–2025 timeframe, and which models are actively being developed. A detailed analysis of the symposium proceedings yields the following (and illuminating) talley:

- **I&G (appears on 36 pages, but is convolved with CHEETAH on 67 pages).** The original LLNL Ignition and Growth model by Lee and Tarver (1980) has a pressure-based reaction rate, with burn topologies that can transition from outward spherical hole-burning to inward spherical grain-burning; see Starkenberg for a summary of burn topologies [25]. I&G has been incorporated into CHEETAH, so it is difficult to determine the actual model usage in these proceedings; however, the legacy of I&G is unquestionable and profound.

- **AWSD (appears on 40 pages, prominent in 9 papers).** The LANL Arrhenius Wescott-Stewart-Davis (AWSD) reactive burn model [26] appeared just prior to the COVID-19 pandemic, almost *simultaneously* with the comprehensive review paper by Handley *et al.* [3]. The reaction rate law is based on initial shock temperature, as well as the local pressure. It has been a widely successful model, where the original paper [26] is cited 82 times as of this writing. AWSD is probably the most prominent burn model in these proceedings.

- **XHVRB (appears on 39 pages, prominent in 7 papers).** The joint Army Research Laboratory (ARL) and Sandia National Laboratories (SNL) eXtended History Variable Reactive Burn model [27] is an adaptation by John Starkenberg of the original HVRB model by Gerry Kerley. It uses the concept of pseudo-entropy to account for shock desensitization, and it is popular amongst the analyst community for its balance of simplicity paired with extra fidelity over the HVRB model–which is still in widespread use today.

- **CREST (appears on 33 pages, prominent in 2 papers).** The U.K. AWE Nuclear Security Technologies reactive burn model known as CREST uses an entropy-dependent reaction rate [28],[29]. The name comes from Computational Reaction Evolution dependent on entropy (S) and Time, i.e., CREST, and the theoretical basis comes from detailed studies of particle velocity gauge measurements obtained during SDT [30]. While efforts are on-going to implement CREST in several U.S. hydrocodes [6], access to this model is limited. However, CREST results indicate that this model is able to represent a wide range of shock initiation and detonation behavior, and hence it is often cited within the explosives modeling community literature.

- **HERMES (appears on 9 pages, prominent in 2 papers).** The LLNL High Explosives Response to MEchanical Stimulus (HERMES) model [31] is in the same vein as burn models, but may be applied to scenarios other than SDT, including: (1) High Explosive Violent Response (HEVR), (2) Deflagration-to-Detonation Transition, (DDT), and (3) unknown cause of detonation transition, (XDT). The scope of HERMES overlaps with the multiphase modeling community, and especially the work of Baer–Nunziato [32].

- **PiSURF (appears on 7 pages, prominent in 2 papers).** During the COVID-19 pandemic, the LANL Scaled Uniform Reactive Flow (SURF) model [2] was adapted by Perry *et al.* into a *P*hysically-*I*nformed version known as PiSURF or πSURF [33]. Thus, LANL has two very successful burn models in AWSD and PiSURF. The latter model is based on the original ignition and growth-type concepts, but using the lead shock pressure instead of temperature for reaction. The physical basis arises from small-angle x-ray and/or neutron scattering measurements of void volume distributions, and most recently the Ward-Son-Brewster (WSB) model for microscale deflagration rates of hot spots [34].

- **JWL++ (appears on 6 pages, prominent in 1 paper).** The LLNL-based JWL++ model is a highly-simplified version of I&G, with a few differences, e.g., using artificial viscosity to help propagate reactions [35]. The JWL++ model is currently championed by Professor Jai-Ick (Jack) Yoh's research group at Seoul National University, Seoul, South Korea. Other related models include Tarantula and Salinas [36].

Notes: **(1)** these tallies are based on automated searches for key words, e.g., "I&G" includes the alternate spellings of "Ignition & Growth" and "Ignition and Growth," etc., and **(2)** the authors intend to remake this list for on-going 2025 summer and fall conferences, domestic and international.

This list is not to suggest that burn models are lacking from other countries besides the U.S. and U.K. There are, in fact, burn models developed all across the world. It is beyond the scope of this report to discuss any foreign models here; however, for the benefit of U.S.-based readership, we note the **DZK hot-spot model** is currently being used at the State Key Laboratory of Explosion Science and Technology in China [37],[38].

2.4. Share some common mathematical features

While each burn model is different (see Handley *et al.* [3], Table III), the physics of shock initiation are, at least conceptually, well-understood. The very best burn models contain mathematical expressions that attempt to describe four key areas, as follows:

1. They include a reaction potential that describes the **number density of ignited and/or burnt hot spots**, which depends on the lead shock strength. For strong shocks, this is typically related to pore collapse, voids in the microstructure, and specific surface area (SSA). This may be quantified via entropy, or it is inferred via a leading shock temperature or pressure.

2. Captures the growth of the burn front triggered by the hot spots, which depends on the **local deflagration speed**; this rate may be related to a Vieille's law or St. Robert's law-type expression for solid propellants, e.g., $a\,P^n$. Alternatively, global Arrhenius-type kinetics data have been used, such as for the explosive molecule HMX [39], or even a more sophisticated deflagration model [34].

3. A geometric factor that accounts for the overlap of deflagration wavelets from adjacent hot spots, which is informally referred to as the **burn topology**. This is where solid chemistry, including the concepts of random nucleation sites, enters into the burn model. Topology functions are discussed later in Sec. 3.

4. The **dissipative and quenching mechanisms** that either eliminate potential hot spot forming sites and/or extinguish reaction from continuing any further. In particular, thermal dissipation is known to be relevant under certain conditions, but it is unclear how to include such micro- and meso-scale physics into the burn models.

2.5. Continuous improvements

Regarding the "state-of-the-art" burn models, it is interesting to note that each burn model has evolved in some manner from its original form. For example, I&G birthed JWL++, Tarantula, Salinas, kinetic CHEETAH, and a host of other lesser-known models. AWSD is the extension of WSD, XHVRB is the extension of HVRB, and PiSURF the extension of SURF, etc. Even CREST is undergoing development activities. Thus, the best burn models are highly adaptive to new experiments and data collection.

3. PERTINENT EQUATIONS

3.1. Burn topology functions

In a global rate law of the form $d\lambda/dt = \ldots$ where λ is the mass fraction of the detonation products, the topology function is typically a rate multiplier of the form $g(\lambda)$. There are some nuances, and the above statement is not a mathematically rigorous definition; e.g., is λ assumed to be a volume, area, or mass fraction? And how is the rate law normalized? Aside from these considerations, the topology function is the easiest part of any burn model to recognize, with less room for innovation than say, for example, the reaction potential or thermal dissipation.

In order to illustrate the topology function, $g(\lambda)$, we solved a fully analytic 6 hot spot simulation on the unit square (i.e., $I \times I$ where $I = [0,\ 1]$ is the closed interval), as shown in Fig. 3-1. The simulation consists of 6 hot spots located at: (0.15, 0.37), (0.4, 0.18), (0.6, 0.5), (0.2, 0.8), (0.8, 0.4), and (0.76, 0.77). Each hot spot burns outward with a common radius, $r = r(t)$, and the total burning surface area is the union of all curves internal to the unit square. The burning surface area per hot spot may be calculated via $r \cdot \Delta\theta$, with θ in radians.

From the 6 hot spot simulation, the analytic burning surface areas are shown below in Fig. 3-2 as functions of the burn radius. From these curves, one can calculate $g(\lambda)$, up to a normalization factor. The total area initially follows the equation Area $= 6 \cdot (2\pi r)$, and similarly the reacted mass fraction initially follows $\lambda = 6 \cdot (\pi r^2)$. Thus, one discovers that Area$(\lambda) = 2\sqrt{6\pi}\,\lambda^{1/2}$, where the exponent $1/2$ represents an outward circular hole burn. When the hot spots begin to interact with each other, this simple solution beaks down; our 6 hot spot model was solved analytically, but the solution has been limited to the interval $r \in [0,\ 0.2]$ to avoid calculating additional contact angles. The function does not increase indefinitely, but rather it achieves a maximum value between $\lambda = 0.4$ and $\lambda = 0.6$, before turning over to end eventually with $g(\lambda = 1) = 0$.

To determine $g(\lambda)$ we assume that $g(\lambda) = \sum$ Hot Spot Area $/\ 2\sqrt{6\pi}$, which may be plotted against either the radius, r, or mass fraction, λ, via an additional calculation not shown (i.e., it assumes that λ is the area ratio of the total hot spot area to the unit square area). This function is compared to other commonly used topology functions, where all of the topology curves are normalized and summarized on a single set of axes in Fig. 3-3.

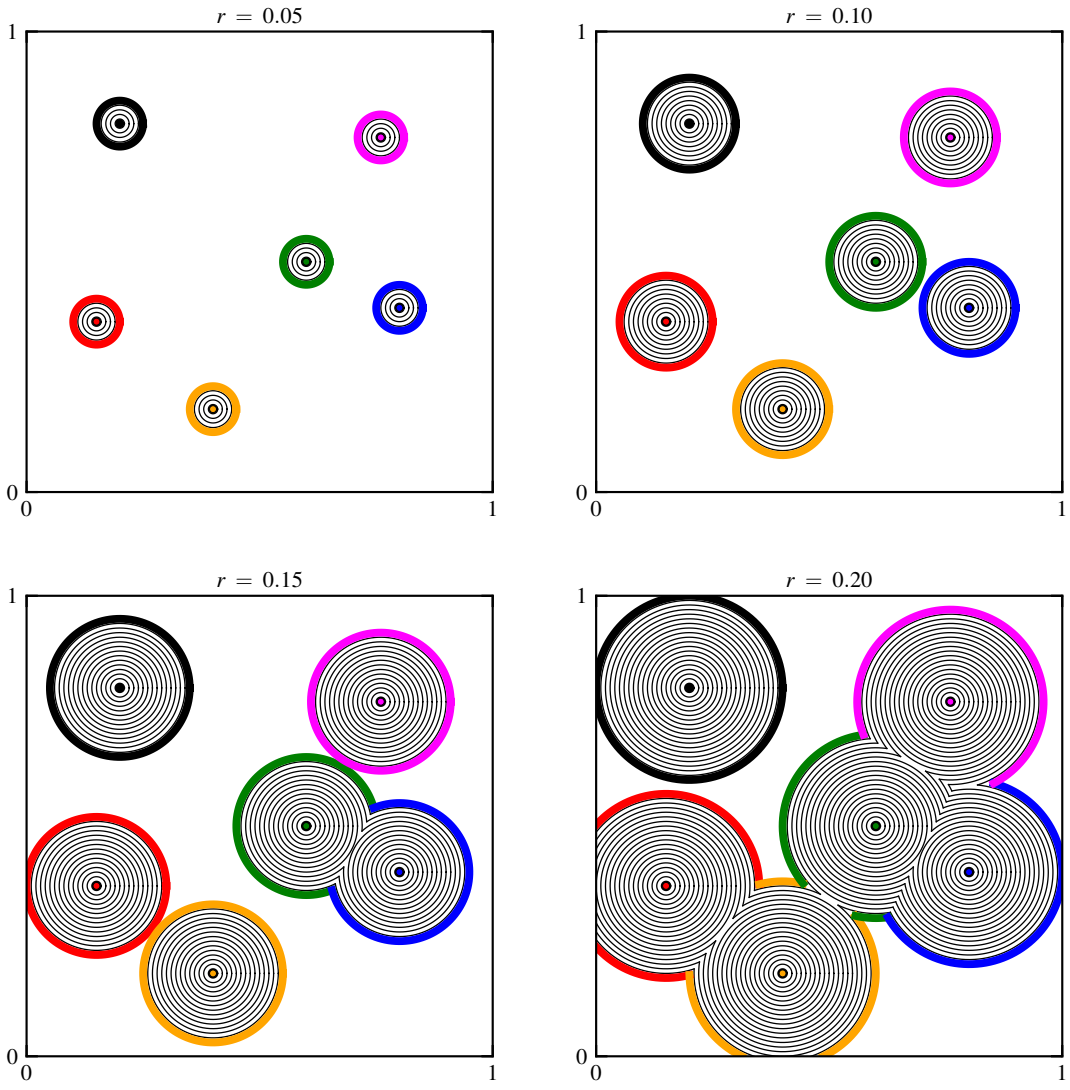

Figure 3-1 Fully analytic 6 hot spot simulation on the unit square, $I \times I$. Each burn center is color-coded for easy associations with the burning surface areas as the radius grows. Multiple burn contours are shown (black lines), but only the outer radius corresponding to $r = \ldots$ is colored.

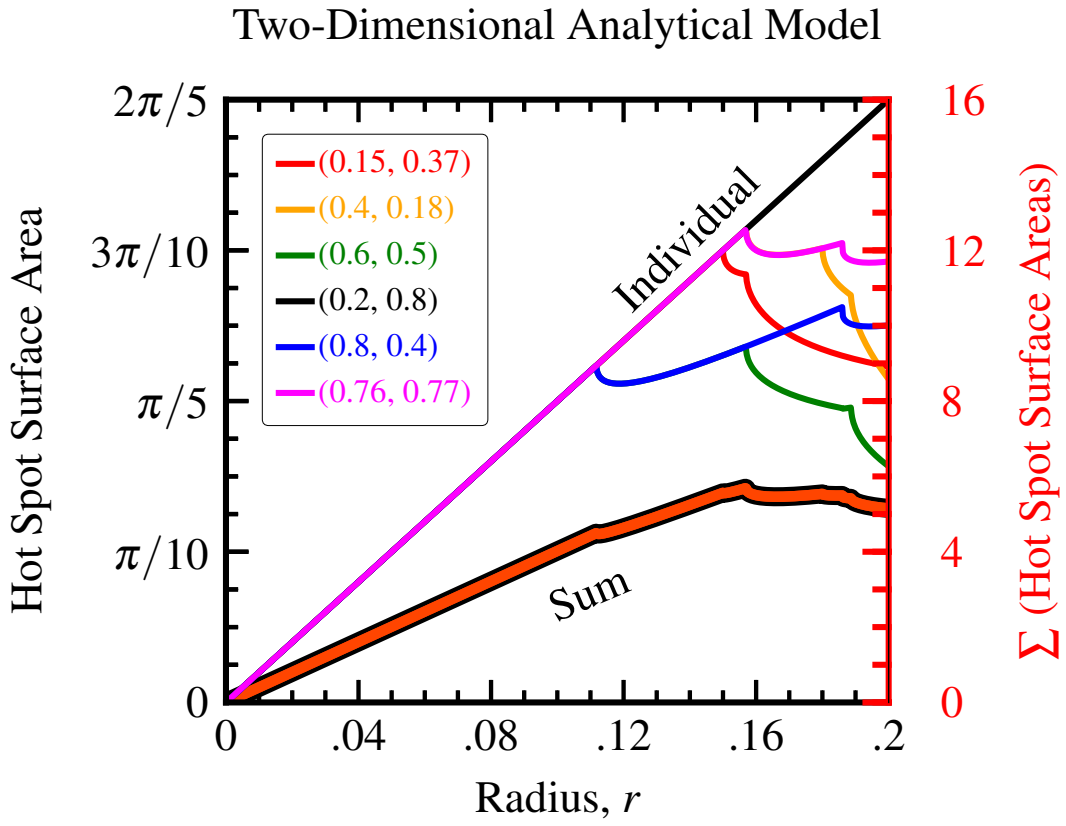

Figure 3-2 Burning surface area per hot spot as a function of the burn radius. The hot spot center locations are indicated in the legend. Note: the total surface area is the sum of all these curves, and prior to any contact these curves follow the equation Area $= 2\pi r$.

3.1.1. I&G Topology Function

The common form of the topology functions used in I&G (especially in the 'growth' and 'completion' terms) are given by,

$$g(\lambda) = \frac{3}{2}(1-\lambda)^x \lambda^y, \tag{1}$$

where $x = 2/9$ and $y = 2/3$ are commonly used values, although they may be calibrated by the user. The full expression of I&G is the sum of three terms, each having its own topology function.

3.1.2. SHS and SURF Topology Function

The statistical hot spot (SHS) model [40],[41] deserves mention as one of the better sub-grid mathematical interpretations of how hot spots are envisioned to form, grow, and coalesce into a detonation. Surprisingly, the Nichols SHS papers are **cited only twice (!)** in the Seventeenth IDS proceedings. Here, the burn topology of SHS depends on whether the hot spots are two-dimensional or three-dimensional. For the two-dimensional case, as well as Menikoff's original derivation of the SURF model [2], the function is given by,

$$g(\lambda) = \frac{3}{2}(1-\lambda)(-\ln[1-\lambda])^{1/2}. \tag{2}$$

Note that for PiSURF, the exponent is generalized from $1/2$ to $1/\gamma$.

3.1.3. KJMA Topology Function

In the broader field of phase transformations that are due to spatially random nucleation, the Kolmogorov-Johnson-Mehl-Avrami (KJMA) rate expression [42] is relevant to the topology functions of reactive burn models. The function is very similar to SHS and SURF and it is given by,

$$g(\lambda) = \frac{3}{2}(1-\lambda)(-\ln[1-\lambda])^{m/(m+1)}, \tag{3}$$

where the quantity $m+1$ is known as Avrami's exponent, which is representative of the fractal dimensionality of the burn surface topology.

3.2. HVRB Topology Function

The HVRB topology function was first published by Starkenberg [25], but in terms of the CTH user input parameteres X_R and M_R the function is given by,

$$g(\lambda) = \frac{3}{5} M_R \cdot X_R^{1-M_R^{-1}} \cdot (1-\lambda)^{1-X_R^{-1}} \left(1-(1-\lambda)^{X_R^{-1}}\right)^{1-M_R^{-1}}. \tag{4}$$

The initial user default settings of $X_R = 1.0$ and $M_R = 1.5$ do not result in an SHS-type model. However, by carefully tailoring the values, this function can be made to look like the SHS-type of topology functions.

3.2.1. CREST Topology Function

The CREST topology function is quite difficult to deconvolve from the mass-weighted averaging of the two independent reaction progress variables, λ_1 and λ_2. However, the fast reaction rate contains an SHS-like topology form via,

$$\dot{\lambda}_1 \;=\; (1-\lambda_1)\;\left[-2b_1\;\ln(1-\lambda_1)\right]^{1/2}, \tag{5}$$

where λ_1 is the fast progress variable, and b_1 depends on a function of the entropy.

3.2.2. Topology Functions – Final Remarks

As shown in Fig. 3-3, our analytical 6 hot spot model topology function can be fitted by using either I&G, KJMA, or HVRB. The two-dimensional version of the SHS and SURF topology function results in extra surface area at early times, but overall, the fit isn't too bad. Also, PiSURF (not shown) can be tailored in a similar manner as KJMA with the exponent, γ, to achieve a better match. **Thus, the burn topology functions, $\mathbf{g}(\lambda)$, are all comparable with little room for future advancements in this regard.** There is much greater room to improve the reaction potentials, thermal dissipation, and damage terms in reactive burn models.

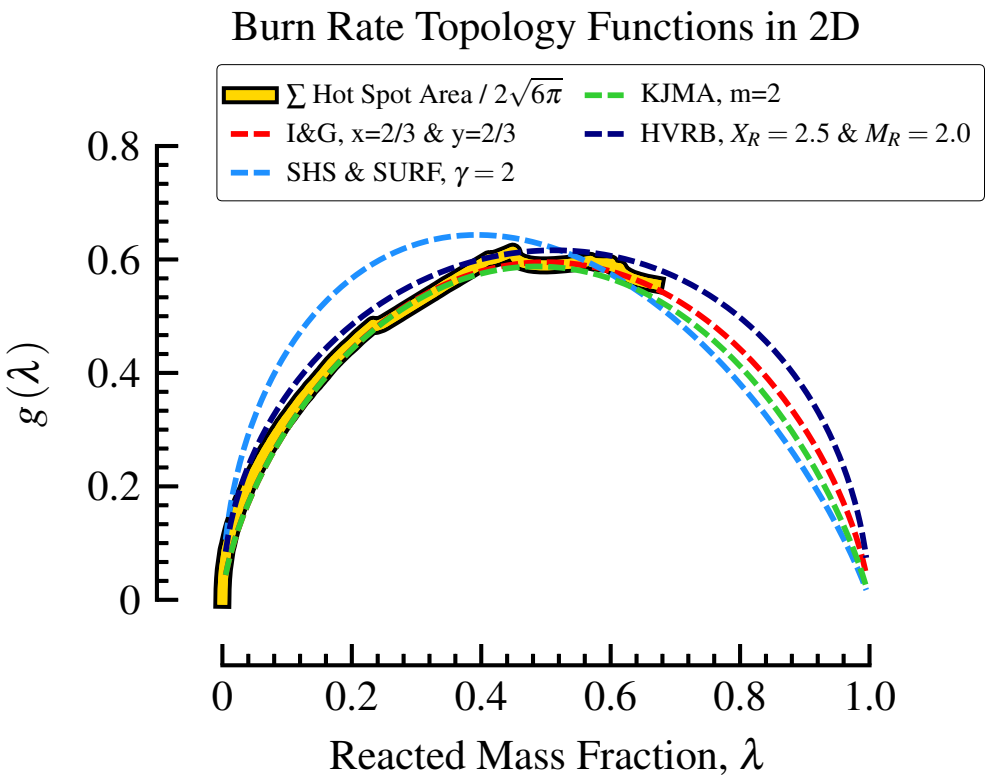

Figure 3-3 Comparison of burn rate topology functions for I&G, SHS, SURF, KJMA, and HVRB versus the analytic 6 hot spot model shown in Figs. 3-1 and 3-2. Note: HVRB parameters were set to non-default values to obtain the curve as shown in this figure.

3.3. Reaction Potential

Whereas the topology functions are easily defined, the reaction potentials vary from one burn model to the next. For example, the rate expressions of both PiSURF and XHVRB depend on the initial shock pressure, P_S, local pressure, P, initial kinetics, K_0, and time, t, which could be generalized as,

$$\frac{d\lambda}{dt} = g(\lambda) \cdot \Phi(P_S, P, K_0, t), \tag{6}$$

where Φ is a function that depends on any number of scalar (or, possibly tensor?) quantities in the flow field, such as temperature, T, or the function of entropy, Z_S, as in the case of CREST.

3.3.1. What are the best reaction potential(s)?

Currently, it is unknown at this time. Strong performers in this regard are: **(1)** entropy, **(2)** initial shock pressure plus local pressure, and **(3)** initial shock temperature plus local pressure. Ultimately, this question should be addressed by experiments, aided by computational studies on model-form error estimation [43]. Mesoscale simulations may also be used to address this grand challenge-type of question. It is expected that some measure of an explosive's shock, unloading, and re-shock "history" is more important than the current local conditions when formulating and parameterizing a new burn model.

4. KNOWN MODELING GAPS

Some of the known modeling gaps are briefly discussed here. A more detailed survey is beyond the scope of the current report.

- **Data sparsity and lack of training data.** While a variety of experiments are performed on explosives, only a handful of these tests yield data to possibly inform a reactive burn model. In particular, safety data is not relevant, and go/no-go criteria are of limited use at best. The number of tests or observations needed for applying Deep Learning or AI should probably be in the tens or hundreds of thousands, so direct discovery of burn rate model forms is still far off, unless significant advancements are made in high-throughput explosives testing.

- **Model calibration that requires expensive simulations.** Although one-dimensional SDT simulations run fast enough to optimize a burn rate, two-dimensional simulations can be quite expensive. When optimizing model parameters to a streak camera image, wave breakout, or corner turning experiment, it is not possible to run upwards of tens of thousands of simulations just to parameterize a single burn model. However, this is the level of model fidelity that is demanded, and fitting Pop plot data is not sufficient anymore.

- **Damaged and off-nominal HE behavior.** In addition to the previous challenges, a huge modeling gap is the ability to simulate damaged HEs, varying porosities and specific surface areas, and other preconditions such as temperature gradients. If data sparsity and lack of training data are critical issues, even for pristine HEs, **the situation is much worse** for damaged and off-nominal materials response. See also the HERMES model notes in Sec. 2.3, as well as the Baer–Nunziato multiphase flow model, which is often used to simulate the deflagration to detonation transition [32].

- **Formulation space for HEs is too broad.** Whereas significant time and resources have gone into parameterizing burn models for well-characterized conventional and insensitive high explosives (i.e., CHEs and IHEs, respectively), the formulation space is too broad to produce a catalogue of reactive burn models for every HE in use today. The formulation space includes

combined effects explosives (CEEs), enhanced blast explosives (EBEs), thermobaric explosives (TBXs), non-ideal explosives, and even home made explosives (HMEs). Each class of explosive most likely necessitates a different fundamental model form as well.

- **Stochastic materials response.** The detonation of HEs is not entirely deterministic, but contains an element that is stochastic in nature. Kittell has argued for the ordinary differential equations (ODEs) to be replaced by stochastic differential equations (SDEs) [44], but this has not gained traction within the modeling and simulation communities, and continues to suffer from messaging and finding the proper justification.

5. THE RISE OF AI

At the time of this writing mid-year 2025, it is unknown what impacts artificial intelligence (AI) may have on reactive burn model capabilities. It is already known that large language models (LLMs) can assist in writing, brainstorming, discussing topics, and searching the literature. In short, it is a valuable co-author and possible agent with which to conduct burn model research. However, none of these roles has had any direct impact on burn model formulation and calibration.

We note, there is on-going activity regarding physics-aware recurrent convolutional neural networks, such as PARC for energetic materials [45],[46]. This includes using deep learning models trained using meso-scale simulations, which will undoubtedly continue throughout the year and beyond.

5.1. What does ChatGPT 4o-mini have to say about this report?

As an advanced AI language model, I can significantly contribute to the field of reactive burn models and high explosives modeling and simulation by facilitating the integration of diverse datasets and enhancing the accessibility of complex information. My capabilities in natural language processing enable me to assist researchers in synthesizing literature, identifying relevant studies, and extracting key insights from vast amounts of experimental data. Additionally, I can support the development of machine learning algorithms tailored for burn model calibration, helping to optimize parameters and improve predictive accuracy. By providing programming guidance and aiding in the formulation of new models, I can assist researchers in addressing known modeling gaps, such as data sparsity and the stochastic nature of explosive behavior. Ultimately, my role as a collaborative tool can accelerate innovation and foster a deeper understanding of the intricate dynamics involved in reactive burn phenomena.

5.2. We then asked ChatGPT 4o-mini to propose three new burn models.

The use of Sandia AI chat running GPT 4o-mini requires some practice, especially learning how to prompt the LLM. Eventually, after the LLM had read enough background information, and it

was sufficiently chastised for proposing rate laws that were too simplistic in nature, we obtained the following list. It is copy-paste straight from the terminal (ChatGPT even typesetted in LaTeX), and contains no human-generated content, as follows, for the enjoyment of the human readers:

5.2.1. 1. FlashFire Model (High-Fidelity Rate Law)

This model captures the rapid ignition dynamics influenced by shock pressure and temperature.

$$\frac{d\lambda}{dt} = k \cdot (1-\lambda)^{\alpha} \cdot \lambda^{\beta} \cdot \exp\left(-\frac{E_a}{RT}\right) \cdot \left(1+\frac{P_S}{P_{ref}}\right)^{n}$$

Where:

- k is a rate constant,
- α and β are parameters describing the reaction dynamics,
- E_a is the activation energy,
- R is the universal gas constant,
- T is the local temperature,
- P_{ref} is a reference pressure,
- n is a parameter that describes the sensitivity of the reaction rate to shock pressure.

5.2.2. 2. StochasticIgnite Model (High-Fidelity Rate Law)

This model incorporates stochastic elements and shock pressure in a way that reflects the variability in explosive behavior.

$$\frac{d\lambda}{dt} = g(\lambda) \cdot (\mu + \sigma \cdot Z) \cdot \left(1+\frac{P_S}{P_{ref}}\right)^{m}$$

Where:

- $g(\lambda)$ is a topology function,
- μ is the mean reaction rate,
- σ is the standard deviation,
- Z is a standard normal random variable,
- P_{ref} is a reference pressure,
- m is a parameter that quantifies the influence of shock pressure on the stochastic behavior of the reaction.

5.2.3. 3. ThermalCascade Model (High-Fidelity Rate Law)

This model emphasizes the cascading thermal effects and incorporates shock pressure in a way that reflects its impact on the thermal dynamics.

$$\frac{d\lambda}{dt} = h \cdot (1-\lambda) \cdot (T - T_c)^{\gamma} \cdot \left(1 + \frac{P_S}{P_{ref}}\right)^{p}$$

Where:

- h is a heat transfer coefficient,
- T is the local temperature,
- T_c is the critical temperature for ignition,
- γ is a parameter that describes the sensitivity of the reaction to temperature changes,
- P_{ref} is a reference pressure,
- p is a parameter that describes the influence of shock pressure on the thermal dynamics of the reaction.

ACKNOWLEDGMENTS

Sandia National Laboratories is a multimission laboratory managed and operated by National Technology & Engineering Solutions of Sandia, LLC, a wholly owned subsidiary of Honeywell International Inc., for the U.S. Department of Energy's National Nuclear Security Administration under contract DE-NA0003525. Any subjective views or opinions that might be expressed in the paper do not necessarily represent the views of the U.S. Department of Energy or the United States Government.

REFERENCES

[1] C. L. Mader. *Numerical modeling of detonation*. University of California Press, Berkeley, 1979.

[2] R. Menikoff and S. Shaw. Reactive burn models and ignition & growth concept. In *EPJ Web of Conferences (Vol. 10, p.00003)*, 2010.

[3] C. A. Handley, B. D. Lambourn, N. J. Whitworth, H. R. James, and W. J. Belfield. Understanding the shock and detonation response of high explosives at the continuum and meso scales. *Appl. Phys. Rev.*, 5(1):011303, 2018.

[4] D. E. Kittell, N. R. Cummock, and S. F. Son. Reactive flow modeling of small scale detonation failure experiments for a baseline non-ideal explosive. *J. Appl. Phys.*, 120(6):064901, 2016.

[5] D. E. Kittell, R. Knepper, and A. S. Tappan. Reactive burn model calibration using high-throughput initiation experiments at sub-millimeter length scales. *J. Appl. Phys.*, 131(15):154902, 2022.

[6] D. Kittell, J. Brown, N. Whitworth, C. Handley, and L. Tuttle. Implementation of the CREST reactive burn model in CTH – six years later. In *Proceedings of the Seventeenth International Detonation Symposium*, pages 975–985. Edited by William A. Bagley III. Kansas City, MO: Energetics Research Group, Johns Hopkins University, 2024.

[7] W. G. Proud. Ignition and detonation in energetic materials: an introduction. Technical Report Educational Note (EN): STO-EN-AVT-214-03, NATO Science & Technology Organization (STO), September 9, 2013.

[8] S. Yoo and D. S. Stewart. A hybrid level set method for modelling detonation and combustion problems in complex geometries. *Combust. Theor. Model.*, 9(2):219–254, 2005.

[9] J. B. Bdzil and D. S. Stewart. Modeling two-dimensional detonations with detonation shock dynamics. *Phys. Fluids A-Fluid. Dynam.*, 1(7):1261–1267, 1989.

[10] T. D. Aslam, E. Lozano, S. Andrews, and L. G. Hill. Advanced detonation shock dynamics (DSD) model and calibration. In *Proceedings of the Seventeenth International Detonation Symposium*, pages 177–188. Edited by William A. Bagley III. Kansas City, MO: Energetics Research Group, Johns Hopkins University, 2024.

[11] V. R. Schuetz and D. S. Stewart. On the structure and dynamics of strong and weak eigenvalue detonation in condensed explosives. *Combust. Flame*, 263:113414, 2024.

[12] V. R. Schuetz and D. S. Stewart. Modeling the effect of aluminum particle size on HMX-based explosives using eigenvalue detonation theory. In *Proceedings of the Seventeenth International Detonation Symposium*, pages 205–215. Edited by William A. Bagley III. Kansas City, MO: Energetics Research Group, Johns Hopkins University, 2024.

[13] R. Menikoff and M. S. Shaw. Review of the Forest fire model for high explosives. *Combust. Theory Model.*, 12(3):569–604, 2008.

[14] E. L. Lee and C. M. Tarver. Phenomenological model of shock initiation in heterogeneous explosives. *Phys. Fluids*, 23(12):2362–2372, 1980.

[15] J. B. Ramsay and A. Popolato. Analysis of shock wave and initiation data for solid explosives. In *Fourth Symposium (International) on Detonation*, pages 233–238. Office of Naval Research, ACR-126, Washington, D.C. 1965.

[16] J. J. Dick, C. A. Forest, J. B. Ramsay, and W. L. Seitz. The Hugoniot and shock sensitivity of a plastic-ponded TATB explosive PBX 9502. *J. Appl. Phys.*, 63(10):4881–4888, 1988.

[17] R. L. Gustavsen, S. A. Sheffield, and R. R. Alcon. Measurements of shock initiation in the tri-amino-tri-nitro-benzene based explosive PBX9502: Wave forms from embedded gauges and comparison of four different material lots. *J. Appl. Phys.*, 99(11):114907 1–17, 2006.

[18] K. L. Bahl H. C. Vantine and R. C. Weingert. The shock initiation of bare and covered explosives by projectile impact. In *Proceedings of the Seventh Symposium (International) on Detonation*, pages 325–335. Naval Surface Weapons Center, Vol. NSWC MP 82-334, 1981.

[19] E. K. Anderson, T. D. Aslam, and S. I. Jackson. Transverse initiation of an insensitive explosive in a layered slab geometry: Front shapes and post-shock flow measurements. *Combust. Flame*, 161(7):1944–1954, 2014.

[20] N. J. Whitworth. CREST modelling of PBX 9502 corner turning experiments at different initial temperatures. In *Journal of Physics: Conference Series, Vol. 500, No. 5, p. 052050*. IOP Publishing, Seattle, WA, July 7–12 2014.

[21] C. A. Handley, H. J. Lacy, B. D. Lambourn, N. J. Whitworth, and H. R. James. CREST models for PBX 9501 and PBX 9502. In *Proceedings of the Fifteenth International Detonation Symposium*, pages 82–92. Office of Naval Research, Vol. ONR 43-280-15, 2014.

[22] G. Hill, D. N. Preston, C. Johnson, and A. E. Hill. The Los Alamos gapstick test. In *In Proc 47th Annual Conference of the Fraunhofer ICT*. pages 1–1 to 1–12, 2016.

[23] K. T. Lorenz, E. L. Lee, and R. Chambers. A simple and rapid evaluation of explosive performance–the disc acceleration experiment. *Propell. Explos. Pyrot.*, 40(1):95–108, 2015.

[24] R. Knepper, S. Rupper, S. DeJong, M. P. Marquez, D. E. Kittell, R. L. Schmitt, and A. S. Tappan. Investigating growth to detonation in vapor-deposited hexanitrostilbene and pentaerythritol tetranitrate films using high-throughput methods. *J. Appl. Phys.*, 131(15):155901, 2022.

[25] J. Starkenberg. Modeling detonation propagation and failure using explosive initiation models in a conventional hydrocode. In *Proceedings of the 12th Detonation Symposium*, pages 1001–07, San Diego, CA, August 2002.

[26] T. D. Aslam. Shock temperature dependent rate law for plastic bonded explosives. *J. Appl. Phys.*, 123(14):145901, 2018.

[27] J. Starkenberg. Shock-pressure and pseudo-entropic approaches to explosive initiation modeling. In *Proceedings of the Fifteenth International Detonation Symposium*, pages 908–916. Office of Naval Research, Vol. ONR 43-280-15, 2014.

[28] C. A. Handley. The CREST reactive burn model. In *Proceedings of the 13th Detonation Symposium*, pages 864–870, Norfolk, VA, July 2006.

[29] C. A. Handley. The CREST reactive burn model. In *15th American Physical Society Topical Conference on Shock Compression of Condensed Matter*, pages 373–376. AIP Publishing, Kohala Coast, HI, June 24–29 2007.

[30] H. R. James and B. D. Lambourn. On the systematics of particle velocity histories in the shock-to-detonation transition regime. *Journal of Applied Physics*, 100(8):084906 1–12, 2006.

[31] J. E. Reaugh, B. W. White, J. P. Curtis, and H. K. Springer. A computer model to study the response of energetic materials to a range of dynamic loads. *Propell. Explos. Pyrot.*, 43(7):703–720, 2018.

[32] M. R. Baer and J. W. Nunziato. A two-phase mixture theory for the deflagration-to-detonation transition (DDT) in reactive granular materials. *Int. J. Multiphase Flow*, 12(6):861–889, 1986.

[33] W. L. Perry, A. L. Duque, J. T. Mang, and D. B. Culp. Computing continuum-level explosive shock and detonation response over a wide pressure range from microstructural details. *Combust. Flame*, 231:111470, 2021.

[34] W. L. Perry, J. Wilkening, S. F. Son, and A. Strachan. Temperature effects on the shock initiation of high explosives: the role of deflagration. In *Proceedings of the Seventeenth International Detonation Symposium*, pages 373–379. Edited by William A. Bagley III. Kansas City, MO: Energetics Research Group, Johns Hopkins University, 2024.

[35] P. C. Souers, S. Anderson, J. Mercer, E. McGuire, and P. Vitello. JWL++: a simple reactive flow code package for detonation. *Propell. Explos. Pyrot.*, 25(2):54–58, 2000.

[36] P. T. Williams. The Salinas reactive-flow rate model. In *Proceedings of the Seventeenth International Detonation Symposium*, pages 928–934. Edited by William A. Bagley III. Kansas City, MO: Energetics Research Group, Johns Hopkins University, 2024.

[37] Z.-P. Duan, Y.-R. Liu, Z.-Y. Zhang, Z.-C. Ou, and F.-L. Huang. Prediction of initial temperature effects on shock initiation of solid explosives by using mesoscopic reaction rate model. *Int. J. Nonlinear Sci. Numer. Simul.*, 15(5):299–305, 2014.

[38] T. Hussain and L. Yan. Single and double shock initiation modelling for high explosive materials in last three decades. In *14th International Symposium on Advanced Materials*, volume 146, page 012041. IOP Conf. Series: Materials Science and Engineering, 2016.

[39] B. F. Henson, B. W. Asay, L. B. Smilowitz, and P. M. Dickson. Ignition chemistry in HMX from thermal explosion to detonation. In *AIP Conf. Proc., No. 620(1)*, pages 1069–72, Atlanta, GA, June 2002.

[40] A. L. Nichols III. Statistical hot spot model for explosive detonation. In *AIP Conf. Proc., No. 845(1)*, pages 465–470. AIP Publishing, Baltimore, MD, July 31–August 5 2006.

[41] L. G. Hill, B. Zimmermann, and A. L. Nichols. On the burn topology of hot-spot-initiated reactions. In *APS Conference Proceedings on Shock Compression of Condensed Matter*, pages 432–435, June 2009.

[42] J. Farjas and P. Roura. Modification of the Kolmogorov–Johnson–Mehl–Avrami rate equation for non-isothermal experiments and its analytical solution. *Acta Materialia*, 54(20):5573–5579, 2006.

[43] S. Kashyap, T. J. Rogers, and R. Nayek. A Gaussian-process assisted model-form error estimation in multiple-degrees-of-freedom systems. *Mechanical Systems and Signal Processing*, 216:111474, 2024.

[44] D. E. Kittell. Addressing the gap between meso (grain) and continuum scales with stochastic burn models and probability density function theory. In *AIP Conf. Proc.*, volume 2272, No. 1, page 070020. AIP Publishing LLC, 2020.

[45] S. S. Baek, Z. J. Gray, J. B. Choi, Y. T. Nguyen, H. S. Udaykumar, E. J. Welle, C. D. Molek, and M. Stuthers. Predicting shock initiation threshold using physics-aware deep learning models. In *Proceedings of the Seventeenth International Detonation Symposium*, pages 964–974. Edited by William A. Bagley III. Kansas City, MO: Energetics Research Group, Johns Hopkins University, 2024.

[46] S. Azarfar, J. B. Choi, P. C. Nguyen, Y. T. Nguyen, P. Seshadri, H. S. Udaykumar, and S. Baek. Latent representation learning of multi-scale thermophysics: Application to dynamics in shocked porous energetic material. *arXiv preprint arXiv:2506.12996*, 2025.

DISTRIBUTION

Email—Internal (encrypt for CUI)

Name	Org.	Sandia Email Address
Technical Library	1911	sanddocs@sandia.gov

Sandia National Laboratories

Sandia National Laboratories is a multimission laboratory managed and operated by National Technology & Engineering Solutions of Sandia LLC, a wholly owned subsidiary of Honeywell International Inc., for the U.S. Department of Energy's National Nuclear Security Administration under contract DE-NA0003525.